Peptide Therapeutics

Deutsche Ausgabe: DOI: 10.1002/ange.201502646
Internationale Ausgabe: DOI: 10.1002/anie.201502646

Targeting the Two Oncogenic Functional Sites of the HPV E6 Oncoprotein with a High-Affinity Bivalent Ligand**

*Juan Ramirez, Juline Poirson, Clémence Foltz, Yassmine Chebaro, Maxime Schrapp, Amandine Meyer, Anaëlle Bonetta, Anne Forster, Yves Jacob, Murielle Masson, François Deryckère, and Gilles Travé**

Abstract: *The E6 oncoproteins of high-risk mucosal (hrm) human papillomaviruses (HPVs) contain a pocket that captures LxxLL motifs and a C-terminal motif that recruits PDZ domains, with both functions being crucial for HPV-induced oncogenesis. A chimeric protein was built by fusing a PDZ domain and an LxxLL motif, both known to bind E6. NMR spectroscopy, calorimetry and a mammalian protein complementation assay converged to show that the resulting PDZ-LxxLL chimera is a bivalent nanomolar ligand of E6, while its separated PDZ and LxxLL components are only micromolar binders. The chimera binds to all of the hrm-HPV E6 proteins tested but not to low-risk mucosal or cutaneous HPV E6. Adenovirus-mediated expression of the chimera specifically induces the death of HPV-positive cells, concomitant with increased levels of the tumour suppressor P53, its transcriptional target p21, and the apoptosis marker cleaved caspase 3. The bifunctional PDZ-LxxLL chimera opens new perspectives for the diagnosis and treatment of HPV-induced cancers.*

Papillomaviruses (PVs) infect the cutaneous and mucosal epithelia of vertebrates.[1] Whereas most PVs are benign, a subset of "high-risk" mucosal human PV types (hrm-HPVs) induce cervical cancer[2] and a significant proportion of head and neck cancers.[3] HPV 16 is the most prevalent and best studied hrm-HPV type. HPV carcinogenesis is primarily linked to two PV oncoproteins, E6 and E7.[4] hrm-HPV E6 recruits the ubiquitin ligase E6AP and the tumour suppressor P53, which leads to ubiquitin-mediated degradation of P53.[5] This dramatically reduces P53 protein levels in HPV-infected cells, thereby disrupting the pro-apoptotic and genome watchdog functions of P53. In this process, E6 binds within E6AP an acidic leucine-rich motif containing an LxxLL consensus sequence.[6] The X-ray crystallography structure of the E6/E6AP complex has shown that E6 captures the motif within a conserved basic–hydrophobic pocket.[7] Hrm-HPV E6 also binds to and sometimes promotes the degradation of several PDZ-containing cellular proteins, which regulate cell–cell adhesion, cell polarity, and apoptosis. Hrm-HPV E6 captures PDZ domains by means of a short PDZ binding motif (PBM), which is situated at the extreme C terminus of E6.[8] Several structures of E6/PDZ complexes have been solved[9].

E6 thus possesses two interaction surfaces responsible for its two best-described oncogenic activities. We exploited our recent structural insights into both activities[7,9a] to build a heterobivalent E6-binding construct to simultaneously target both interaction surfaces. We designed a chimeric PDZ-LxxLL fusion protein (Figure S1 in the Supporting Information) comprising the MAGI1 PDZ2 domain (the second of the six PDZ domains of MAGI1, sometimes named "PDZ1" or "PDZ2/6" in earlier works),[9a] a three-alanine linker, and the E6-binding LxxLL motif of E6AP (sequence: ELTLQELLGEER).[7] By combining our previous structures of the E6/LxxLL complex (PDB ID 4GIZ[7]; Figure 1a) and of the E6/PDZ2 complex (PDB ID 2KPL[9a]; Figure 1b), we built a tridimensional model of the planned PDZ-LxxLL chimera (Figure 1c and the Supporting Information) and of its expected complex with E6 (Figure 1d). In this model, an unfolded 25-residue extension situated at the C terminus of the PDZ2 construct provides, between the folded PDZ core and the LxxLL motif, a natural linker that allows simultaneous binding of the PDZ and LxxLL moieties of one chimera molecule to their respective binding surfaces on one E6 molecule.

[*] Dr. J. Ramirez, J. Poirson, C. Foltz, M. Schrapp, A. Meyer, Dr. A. Bonetta, A. Forster, Dr. M. Masson, Dr. F. Deryckère, Dr. G. Travé
Oncoprotein Team, Équipe Labellisée Ligue 2015
UMR CNRS-UDS 7242
École Supérieure de Biotechnologie de Strasbourg
Boulevard Sébastien Brant, BP 10413, F-67412 Illkirch (France)
E-mail: trave@unistra.fr

Dr. Y. Chebaro
IGBMC
1 rue Laurent Fries, BP 10142, 67404 Illkirch (France)

Dr. Y. Jacob
Institut Pasteur, Unité de Génétique Moléculaire des Virus à ARN
Département de Virologie & UMR CNRS 3569, Paris (France)

[**] This work was supported by institutional support from CNRS, Université de Strasbourg, and grants from Association pour la Recherche contre le Cancer (ARC) (n° 3171), Agence Nationale de la Recherche (ANR-MIME-2007 EPI-HPV-3D), National Institute of Health (NIH grant R01A134737), Ligue contre le Cancer and Alsace contre le cancer. J.R. was supported by ANR grant MIME-2007 EPI-HPV-3D and NIH grant R01A134737. J.P. was supported by a grant of Ligue contre le Cancer. The authors thank Danièle Altschuh, Nicolas Wolff, and all members of the "Oncoproteins" team for helpful discussions and advice.

Supporting information for this article is available on the WWW under http://dx.doi.org/10.1002/anie.201502646.

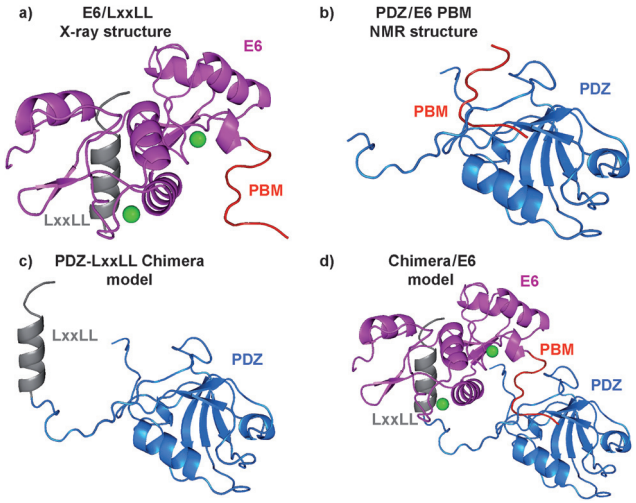

Figure 1. Designing a chimeric bivalent ligand for hrm-HPV E6. a) Crystal structure of the E6/LxxLL complex.[7] The helical LxxLL motif of E6AP (grey) inserts into the LxxLL binding pocket of E6 (purple). The unbound C-terminal PBM of E6 (red) is extended and flexible. b) NMR structure of the MAGI1 PDZ2/E6 PBM complex.[9a] The E6 PBM (red) inserts into the peptide-binding groove of the PDZ domain (blue). c) Model structure of the PDZ-LxxLL chimera. d) Model structure of the chimera bound to E6. The long linker between folded PDZ core and LxxLL motif enables the simultaneous binding of PDZ and LxxLL to E6 PBM and E6 pocket, respectively.

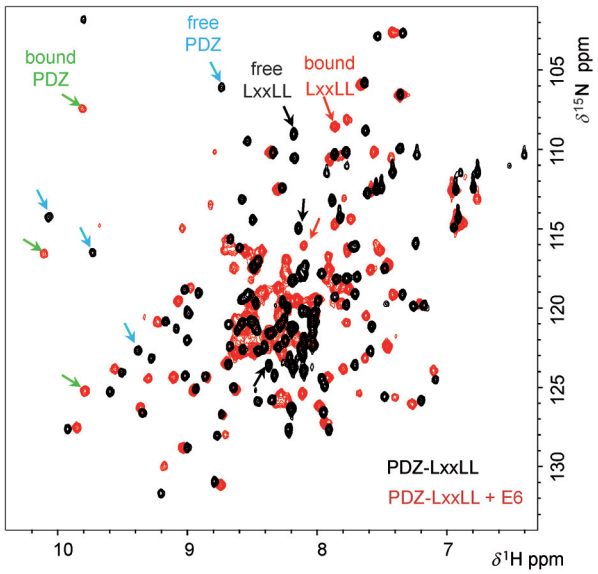

Figure 2. NMR characterization of the PDZ-LxxLL chimera and its interaction with E6. Superimposed HSQC spectra (recorded at 25 °C) of E6-bound PDZ-LxxLL chimera (red) and free PDZ-LxxLL chimera (black). The black, blue, red, and green arrows indicate characteristic signals of free LxxLL, free PDZ, bound LxxLL, and bound PDZ, respectively, as identified by comparing different spectra (see Figures S3, S4).

The PDZ-LxxLL chimera was cloned, bacterially expressed, and purified (Figure S2). The purified construct was highly soluble (up to 1 mM). We used NMR to probe the interaction of a ^{15}N-labelled chimera with unlabeled E6 F47R 4C4S, a soluble mutant of HPV16 E6.[10] The [^{1}H,^{15}N] HSQC spectrum of the E6-bound chimera (Figure 2, red peaks) undergoes dramatic changes as compared to that of the free chimera (Figure 2, black peaks). By comparing the HSQC spectra of free chimera, free PDZ domain, free LxxLL peptide, and chimera or PDZ domain bound to E6 or E6 PBM peptide (Figures S3, S4), we could identify in the spectra of free and E6-bound chimera most of the peaks corresponding to free PDZ, free LxxLL, and the PDZ/PBM and LxxLL/E6 complexes (Figure 2). Therefore, the PDZ and LxxLL moieties of the chimera essentially retain, in their free and bound states, the conformations that they adopt when they are not fused to each other. Altogether, the NMR data show that the chimera is a bifunctional ligand of E6 and interacts with both its LxxLL binding pocket and its PBM.

We used isothermal titration calorimetry (ITC) to titrate the chimera (10 μM) with concentrated E6 (122 μM stock; Figure 3a). E6 bound strongly to the chimera, with a steep exothermic binding curve and $K_d = 10$ nM when assuming a 1:1 binding model. In the same assay conditions, E6 did not detectably bind to the LxxLL peptide (Figure S5b). Only by titrating E6 (50 μM) with concentrated LxxLL peptide (600 μM stock) did we observe a gradual exothermic binding curve ($K_d = 42$ μM; Figure 3b). Finally, titration of PDZ (10 μM) with concentrated E6 (122 μM stock) generated a gradual endothermic binding curve ($K_d = 3.5$ μM; Figure 3c). Therefore, the chimera binds E6 in the nanomolar range, with a 300-fold affinity enhancement compared to the PDZ domain and a 4000-fold enhancement compared to the LxxLL peptide. A breakdown of the thermodynamic parameters (Figure 3d, Table S1 in the Supporting Information) reveals comparable profiles for the E6/LxxLL and E6/chimera interactions. Both display a dominant enthalpic contribution, which is reinforced for the E6/chimera complex, thus resulting in a strong increase in binding free energy. Remarkably, premixing the PDZ domain with the LxxLL peptide prior to titration with E6 did not enhance the affinity of PDZ for E6 (Figure S5c), thus further demonstrating that the strong binding affinity of the chimera for E6 essentially stems from the tethering of the PDZ and LxxLL moieties. The chimera binds E6 not only with high affinity but also with high specificity, as testified by its ability to capture endogeneous E6 from HPV18-positive Hela cells (Figure 3e and Figure S6).

We next investigated the binding of the chimera to E6 proteins from various HPV types. Most wild-type E6 proteins display low solubility, thus hindering their purification for biophysical assays.[11] To circumvent this problem, we measured the E6/chimera interactions directly in mammalian cells by using the split *Gaussia princeps* luciferase complementation assay (GPCA).[12] The assay measures the luminescence produced by the potential interactors fused to complementary luciferase fragments, GL1 and GL2. A normalized luminescence ratio (NLR), computed from the luminescence generated by the potential interacting pair and two controls, serves as a binding signal and informs on the probability p that the interaction is true: for NLR > 3.5, $p > 97.5\%$.[12] The approach was applied to measure the binding of E6 proteins

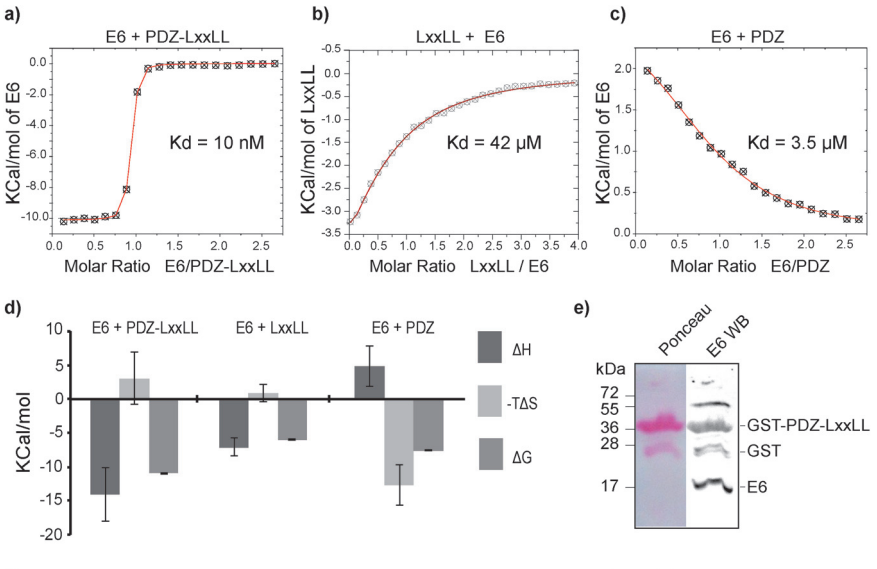

f)

	high-risk mucosal									low-risk mucosal			cutaneous				
HPVs	*33*	*58*	*52*	*18*	*16*	*39*	*35*	*66*	*53*	*6*	*11*	*32*	*1*	*5*	*9*	*38*	*49*
PDZ	730	120	29	160	37	33	2.6	3.9	2.2	0.4	1.0	0.5	0.6	0.4	0.7	0.5	0.6
LxxLL	38	32	100	190	14	26	2.4	3.9	3.5	0.6	0.6	0.9	2.0	0.9	1.1	0.7	0.8
PDZ-LxxLL	3800	2000	1800	1040	1000	440	200	190	180	0.5	0.7	0.9	1.2	0.6	0.6	0.8	0.9

Figure 3. Bivalency provides the chimera with a high affinity for hrm-HPV E6. a) Calorimetric titration of PDZ-LxxLL chimera (10 µM) with E6 (122 µM stock). b) Titration of E6 (50 µM) with LxxLL peptide (600 µM stock). c) Titration of the PDZ domain (10 µM) with E6 (122 µM stock). d) Thermodynamic profiles of E6/chimera, E6/LxxLL, and E6/PDZ interactions. e) Capture of endogeneous HPV18 E6 from Hela cells. A 6-his-GST-PDZ-LxxLL fusion was incubated with Hela cell extracts and double-purified over gluthatione and Ni-chelate affinity columns. Western blotting (WB) with anti-E6 antibody (right) specifically revealed a strong band at the size of E6 (17 kDa). f) Probing the binding of the chimera, PDZ, and LxxLL to 17 distinct HPV E6 proteins by using mammalian GPCA. Red and black numbers indicate NLR values above or below the lower threshold value for high-confidence binding (NLR = 3.5), respectively (see Table S2 for source data).

from 17 HPV types to the LxxLL motif, the PDZ domain, and the PDZ-LxxLL chimera (Figure 3 f and Table S2). HPV16 E6 showed relevant binding signals with both PDZ and LxxLL, and these binding signals further increased 25- and 75-fold when E6 was assayed with the PDZ-LxxLL chimera. Qualitatively, this is in line with the 300-fold and 4000-fold affinity enhancement observed by ITC (Figure 3 a, b and Figure S5). Therefore, the GPCA approach not only detects protein–protein interactions with high confidence; it can also provide qualitative information on binding strengths. Remarkably, all of the E6 proteins from hrm-HPVs (types 16, 18, 33, 35, 39, 52, 53, 58, 66) showed strong binding signals with the chimera, which were highly enhanced compared to the signals they gave with the separate PDZ and LxxLL moieties (Figure 3 f). By contrast, all of the other E6 proteins tested, either from low-risk mucosal HPVs (types 6, 11, 32) or cutaneous HPVs (types 1, 5, 8, 9, 38, 49), showed very low nonsignificant signals with either the chimera, PDZ, or LxxLL. Therefore, the chimera appears to specifically recognize E6 oncoproteins from all hrm-HPV types with a strong binding affinity.

To probe the potential of the chimera as an in vivo inhibitor of E6 oncogenic functions, we transduced Hela (HPV18 positive) and Caski (HPV16 positive) cell lines, which originate from cervical cancers, with a recombinant noninfectious adenovirus (AdV) expressing the chimera. hrm-HPV-positive cells naturally express E6, which interacts with the ubiquitin ligase E6AP to promote the destruction of P53, thereby inactivating apoptotic pathways. The transduced chimera specifically induced the restoration of higher protein levels of P53 and its transcriptional target p21 in HPV-positive cells (Figure 4 a), as well as the cleavage of Caspase 3, a typical marker of apoptosis induction (Figure S7 a). Furthermore, the transduced chimera specifically induced death and detachment of HPV-positive cells (Figure 4 b and Figure S7 b). Surprisingly, the PDZ domain alone also up-regulated P53 and apoptosis markers and induced cell death, albeit less efficiently than the chimera (Figure 4 b and Figure S7 b). Apoptosis has previously been observed in HPV-positive cells overexpressing full-length MAGI1.[13] We hypothesize that PDZ binding to E6 PBM may hinder the E6–E6AP–P53 interaction and/or the subsequent ubiquitination of P53.

In this study, we devised a bifunctional ligand of E6 that simultaneously targets its LxxLL binding pocket and its PDZ-binding motif. The combination of these two micromolar ligands produced a nanomolar ligand. The PDZ and LxxLL moieties appeared conformationally independent in the chimera, whether free or E6-bound (Figure 2 and Figures S3, S4); and the presence of unfused LxxLL peptide did not significantly alter the binding of E6 to the PDZ domain (Figure S5 c and Table S1), thus ruling out strong allosteric coupling between the PDZ- and LxxLL-binding sites of E6. Therefore, the enhanced affinity of the chimera appears mainly attributable to an avidity effect[14] induced by bivalence. Indeed, many biological systems use multivalence to create avidity. This early observation pointed to multivalency as a principle for the design of high-affinity ligands and inhibitors,[15] and this principle was later successfully applied in many different fields.[16] The efficiency of affinity enhancement for a bivalent ligand A-B can be evaluated by computing the effective concentration C_{eff} created by tethering the two sites A and B ($C_{eff} = K_d^A K_d^B / K_d^{A\text{-}B}$).[17] For the PDZ-LxxLL chimera, we obtain a C_{eff} value of approximately 15 mM. This value is in line with that observed for a recently engineered dimeric ligand of Gephyrin (1220-fold affinity increase, $C_{eff} \approx 10$ mM)[18] and

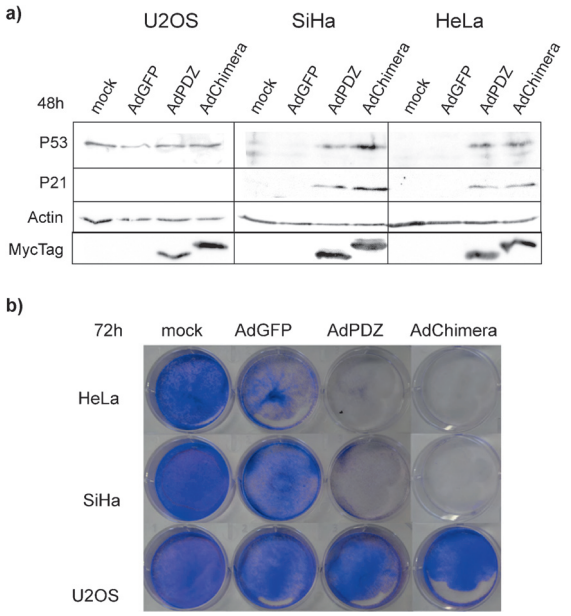

Figure 4. Adenoviral (Ad) expression of the chimera specifically kills HPV-positive cells. a) U20S (HPV−), SiHa (HPV16+), and Hela (HPV18+) cells were transduced for 48 h with adenoviruses expressing GFP, myc-tagged PDZ, or myc-tagged PDZ-LxxLL chimera. The expression of P53, p21, PDZ, and the chimera was analyzed by western blotting with appropriate monoclonal antibodies. P53 and P21 levels specifically increased in the SiHa and HeLa cells transduced with PDZ and the chimera. b) Cells were transduced for 72 h with AdGFP, AdPDZ, and AdChimera. Crystal violet staining reveals massive cell death of HeLa and SiHa cells expressing the chimera and (to a lesser extent) PDZ.

exceeds the C_{eff} value observed for another dimeric ligand targeting the PSD-95 protein (100-fold affinity increase, $C_{eff} \approx 100\ \mu M$).[19]

Being built from fragments of two proteins targeted by all hrm-HPV E6 proteins, the chimera proved to be a universal ligand for hrm-HPV E6 proteins. This is a strong advantage over previously published E6 ligands, including small molecules,[20] antibodies,[21] peptides,[22] and RNA aptamers,[23] which were all developed to target only one particular E6 protein (HPV16 E6). Since E6 is a hallmark of all HPV-positive tumors, the chimera can serve as a diagnostic tool for E6 capture followed by immunodetection, as demonstrated here (Figure 3e). One can also envision the design of fluorescent biosensors derived from the chimera that would directly detect the presence of E6 in extracts.

Since it is composed of host protein fragments, the chimera is likely to be "invisible" to the immune system. It is also expected to be highly selective for viral E6 in the intracellular context because it is very unlikely that any cell protein would combine, like E6, a pocket recognizing both the LxxLL motif of E6AP and a PBM targeting the MAGI1 PDZ2 domain. Since it targets the two regions of E6 required for its oncogenic functions, the chimera represents a promising candidate for therapeutic approaches based on E6 inhibition in HPV-induced tumors. As a proof of concept, the adenovirally expressed chimera specifically induced apoptotic death of HPV-positive cells through the restoration of P53. It will be worth investigating the effect of the chimera in in vivo models of HPV-induced cancers.[24]

Keywords: antitumor agents · human papillomavirus · inhibitors · peptides · protein engineering

How to cite: *Angew. Chem. Int. Ed.* **2015**, *54*, 7958–7962
Angew. Chem. **2015**, *127*, 8069–8073

[1] K. Van Doorslaer, *Virology* **2013**, *445*, 11–20.
[2] H. zur Hausen, *Nat. Rev. Cancer* **2002**, *2*, 342–350.
[3] M. L. Gillison, L. Alemany, P. J. Snijders, A. Chaturvedi, B. M. Steinberg, S. Schwartz, X. Castellsagué, *Vaccine* **2012**, *30*, F34–F54.
[4] R. Ghittoni, R. Accardi, U. Hasan, T. Gheit, B. Sylla, M. Tommasino, *Virus Genes* **2010**, *40*, 1–13.
[5] J. M. Huibregtse, M. Scheffner, P. M. Howley, *EMBO J.* **1991**, *10*, 4129–4135.
[6] S. B. Vande Pol, A. J. Klingelhutz, *Virology* **2013**, *445*, 115–137.
[7] K. Zanier, S. Charbonnier, A. O. Sidi, A. G. McEwen, M. G. Ferrario, P. Poussin-Courmontagne, V. Cura, N. Brimer, K. O. Babah, T. Ansari, I. Muller, R. H. Stote, J. Cavarelli, S. Vande Pol, G. Travé, *Science* **2013**, *339*, 694–698.
[8] M. Thomas, N. Narayan, D. Pim, V. Tomaić, P. Massimi, K. Nagasaka, C. Kranjec, N. Gammoh, L. Banks, *Oncogene* **2008**, *27*, 7018–7030.
[9] a) S. Charbonnier, Y. Nomine, J. Ramirez, K. Luck, A. Chapelle, R. H. Stote, G. Travé, B. Kieffer, R. A. Atkinson, *J. Mol. Biol.* **2011**, *406*, 745–763; b) Y. Liu, G. D. Henry, R. S. Hegde, J. D. Baleja, *Biochemistry* **2007**, *46*, 10864–10874; c) A. Mischo, O. Ohlenschläger, P. Hortschansky, R. Ramachandran, M. Görlach, *PLoS One* **2013**, *8*, e62584; d) Y. Zhang, J. Dasgupta, R. Z. Ma, L. Banks, M. Thomas, X. S. Chen, *J. Virol.* **2007**, *81*, 3618–3626.
[10] K. Zanier, A. O. M. O. Sidi, C. Boulade-Ladame, V. Rybin, A. Chappelle, A. Atkinson, B. Kieffer, G. Travé, *Structure* **2012**, *20*, 604–617.
[11] a) K. Zanier, Y. Nomine, S. Charbonnier, C. Ruhlmann, P. Schultz, J. Schweizer, G. Trave, *Protein Expression Purif.* **2007**, *51*, 59–70; b) K. Zanier, C. Ruhlmann, F. Melin, M. Masson, A. O. M. O. Sidi, X. Bernard, B. Fischer, L. Brino, T. Ristriani, V. Rybin, M. Baltzinger, S. Vande Pol, P. Hellwig, P. Schultz, G. Trave, *J. Mol. Biol.* **2010**, *396*, 90–104.
[12] P. Cassonnet, C. Rolloy, G. Neveu, P. O. Vidalain, T. Chantier, J. Pellet, L. Jones, M. Muller, C. Demeret, G. Gaud, F. Vuillier, V. Lotteau, F. Tangy, M. Favre, Y. Jacob, *Nat. Methods* **2011**, *8*, 990–992.
[13] C. Kranjec, P. Massimi, L. Banks, *J. Virol.* **2014**, *88*, 7155–7169.
[14] a) P. I. Kitov, D. R. Bundle, *J. Am. Chem. Soc.* **2003**, *125*, 16271–16284; b) G. Vauquelin, *Naunyn-Schmiedeberg's Arch. Pharmacol.* **2013**, *386*, 949–962; c) G. Vauquelin, S. J. Charlton, *Br. J. Pharmacol.* **2013**, *168*, 1771–1785.
[15] M. Mammen, S. K. Choi, G. M. Whitesides, *Angew. Chem. Int. Ed.* **1998**, *37*, 2754–2794; *Angew. Chem.* **1998**, *110*, 2908–2953.
[16] C. Fasting, C. A. Schalley, M. Weber, O. Seitz, S. Hecht, B. Koksch, J. Dernedde, C. Graf, E. W. Knapp, R. Haag, *Angew. Chem. Int. Ed.* **2012**, *51*, 10472–10498; *Angew. Chem.* **2012**, *124*, 10622–10650.
[17] a) W. P. Jencks, *Proc. Natl. Acad. Sci. USA* **1981**, *78*, 4046–4050; b) H. X. Zhou, *J. Mol. Biol.* **2003**, *329*, 1–8.
[18] H. M. Maric, V. B. Kasaragod, L. Haugaard-Kedström, T. J. Hausrat, M. Kneussel, H. Schindelin, K. Strømgaard, *Angew. Chem. Int. Ed.* **2015**, *54*, 490–494; *Angew. Chem.* **2015**, *127*, 500–504.

[19] A. Bach, C. N. Chi, G. F. Pang, L. Olsen, A. S. Kristensen, P. Jemth, K. Strømgaard, *Angew. Chem. Int. Ed.* **2009**, *48*, 9685 – 9689; *Angew. Chem.* **2009**, *121*, 9865 – 9869.
[20] a) J. J. Cherry, A. Rietz, A. Malinkevich, Y. Liu, M. Xie, M. Bartolowits, V. J. Davisson, J. D. Baleja, E. J. Androphy, *PLoS One* **2013**, *8*, e84506; b) K. A. Malecka, D. Fera, D. C. Schultz, S. Hodawadekar, M. Reichman, P. S. Donover, M. E. Murphy, R. Marmorstein, *ACS Chem. Biol.* **2014**, *9*, 1603 – 1612.
[21] J. Courtête, A. P. Sibler, G. Zeder-Lutz, D. Dalkara, M. Oulad-Abdelghani, G. Zuber, E. Weiss, *Mol. Cancer Ther.* **2007**, *6*, 1728 – 1735.
[22] K. Zanier, C. Stutz, S. Kintscher, E. Reinz, P. Sehr, J. Bulkescher, K. Hoppe-Seyler, G. Travé, F. Hoppe-Seyler, *PLoS One* **2014**, *9*, e112514.
[23] T. A. Belyaeva, C. Nicol, O. Cesur, G. Travé, G. E. Blair, N. J. Stonehouse, *Cancers* **2014**, *6*, 1553 – 1569.
[24] S. H. Chung, P. F. Lambert, *Proc. Natl. Acad. Sci. USA* **2009**, *106*, 19467 – 19472.

Received: March 22, 2015
Published online: May 26, 2015

